frontiers | Frontiers in Immunology

TYPE Original Research
PUBLISHED 11 January 2024
DOI 10.3389/fimmu.2023.1305976

OPEN ACCESS

EDITED BY
Michail Kotsyfakis,
Foundation for Research and Technology Hellas (FORTH), Greece

REVIEWED BY
Albert Mulenga,
Texas A and M University, United States
Radek Šíma,
Academy of Sciences of the Czech Republic (ASCR), Czechia

*CORRESPONDENCE
Shahid Karim
Shahid.Karim@usm.edu

RECEIVED 02 October 2023
ACCEPTED 22 December 2023
PUBLISHED 11 January 2024

CITATION
Adegoke A, Ribeiro JMC, Smith RC and Karim S (2024) Tick innate immune responses to hematophagy and *Ehrlichia* infection at single-cell resolution.
Front. Immunol. 14:1305976.
doi: 10.3389/fimmu.2023.1305976

Tick innate immune responses to hematophagy and *Ehrlichia* infection at single-cell resolution

Abdulsalam Adegoke[1], Jose M. C. Ribeiro[2], Ryan C. Smith[3] and Shahid Karim[1]*

[1]School of Biological, Environmental, and Earth Sciences, The University of Southern Mississippi, Hattiesburg, MS, United States, [2]Vector Biology Section, Laboratory of Malaria and Vector Research, National Institute of Allergy and Infectious Diseases, National Institutes of Health, Rockville, MD, United States, [3]Department of Plant Pathology, Entomology, and Microbiology, Iowa State University, Ames, IA, United States

Introduction: Ticks rely on robust cellular and humoral responses to control microbial infection. However, several aspects of the tick's innate immune system remain uncharacterized, most notably that of the immune cells (called hemocytes), which are known to play a significant role in cellular and humoral responses. Despite the importance of hemocytes in regulating microbial infection, our understanding of their basic biology and molecular mechanisms remains limited. Therefore, we believe that a more detailed understanding of the role of hemocytes in the interactions between ticks and tick-borne microbes is crucial to illuminating their function in vector competence and to help identify novel targets for developing new strategies to block tick-borne pathogen transmission.

Methods: This study examined hemocytes from the lone star tick (*Amblyomma americanum*) at the transcriptomic level using the 10X genomics single-cell RNA sequencing platform to analyze hemocyte populations from unfed, partially blood-fed, and *Ehrlichia chaffeensis*-infected ticks. The functional role of differentially expressed hemocyte markers in hemocyte proliferation and *Ehrlichia* dissemination was determined using an RNA interference approach.

Results and discussion: Our data exhibit the identification of fourteen distinct hemocyte populations. Our results uncover seven distinct lineages present in uninfected and *Ehrlichia*-infected hemocyte clusters. The functional characterization of *hemocytin*, *cystatin*, *fibronectin*, and *lipocalin* demonstrate their role in hemocyte population changes, proliferation, and *Ehrlichia* dissemination.

Conclusion: Our results uncover the tick immune responses to *Ehrlichia* infection and hematophagy at a single-cell resolution. This work opens a new field of tick innate immunobiology to understand the role of hemocytes, particularly in response to prolonged blood-feeding (hematophagy), and tick-microbial interactions.

KEYWORDS

hemocytes, 10X Genomics, *Amblyomma americanum*, *Ehrlichia chaffeensis*, single cell, RNA-sequencing

Introduction

Hematophagous arthropods and insect vectors transmit numerous pathogenic microbes, including bacteria, viruses, and parasites, posing a significant threat to human and animal health worldwide. These blood-feeding ectoparasites have evolved intricate mechanisms to overcome host immune defenses and ensure successful feeding and pathogen transmission. Understanding the cellular components and dynamics of the tick immune system is essential for unraveling the underlying mechanisms of tick-host interactions and developing effective strategies for controlling tick-borne diseases. The immune cells of arthropods or hemocytes serve as the primary line of defense against invading pathogens. In ticks, these versatile immune cells play a vital role in recognizing, encapsulating, and eliminating pathogens acquired during feeding or through vertical transmission (1–3). Hemocyte mediates several immune processes ranging from phagocytosis, nodulation, melanization, and the release of antimicrobial peptides (4–10).

Tick hemocytes exhibit remarkable heterogeneity and complexity, comprising multiple distinct subpopulations with unique functional attributes. Traditional microscopy approaches have provided valuable insights into the overall composition and morphology of tick hemocytes (9–11), leading to the identification of five types: prohemocytes, plasmatocytes, granulocytes, spherulocytes, and oenocytoids (9–11). Interestingly, several studies have reported fewer hemocyte types in other tick species (12, 13). Transcriptional studies of tick hemocytes (9, 14) have revealed important information regarding the molecular regulation of tick hemocytes during physiological processes such as blood feeding or microbial infection. Nevertheless, these techniques often fail to capture the full spectrum of cellular diversity and functional heterogeneity at the single-cell level, limiting our understanding of the intricate cellular immune responses accompany blood feeding or infection. Single-cell RNA sequencing (scRNA-seq) has redefined our understanding of hemocyte populations in invertebrate models such as *Drosophila* (15–17), mosquito (18–20), silkworm and moth (21, 22), ticks (23) and aquatic invertebrates (24–26). Applying scRNA-seq in these organisms has led to identifying additional hemocyte complexity and cell types when compared to previous classifications (19, 20). In addition, its application has redefined hemocyte complexity in response to pathogen infection (22).

This study presents a comprehensive single-cell characterization of the lone-star tick (*Amblyomma americanum*) hemocytes, aiming to unravel the cellular complexity and functional diversity in response to blood feeding and *Ehrlichia* (E) *chaffeensis* infection for the first time. We identified a higher diversity of hemocyte clusters defined by highly expressed marker genes specific to each cluster when hemocytes from the uninfected cohort were compared to *E. chaffeensis*-infected cohorts. The task of correlating the transcriptomic populations from this study with the morphological populations obtained from microscopy and molecular studies in *A. americanum* is still challenging due to the lack of a genome and limited transcriptome and proteome. However, our findings suggest the presence of highly diverse hemocyte populations in *A. americanum*.

Methods

Tick rearing and generation of Ehrlichia-infected ticks

Fully replete *Amblyomma americanum* nymphs were purchased from the Oklahoma State University's Tick Rearing Facility and maintained at 34°C and 65% RH under 14:10 h L:D photoperiod till needed. *Ehrlichia* infected adult ticks were generated as previously described (27). Briefly, fully engorged nymphs were injected with *E. chaffeensis* (Arkansas strain) using a 32-guage needle fitted to a Hamilton syringe (Hamilton Company, Franklin, MA, USA). All injected ticks were monitored for 25 hours at a temperature of 34°C to remove dead or non-viable nymphs. Viable nymphs were transferred into an incubator maintained at 34°C and 65% RH under 14:10 h L:D photoperiod and monitored until they molted into adult male and females. Adult ticks were fed on sheep and removed at the partially-fed phase (50-100mg). To allow us capture cellular changes throughout feeding, we staggered tick infestation on sheep such that at the point of tick removal, we had ticks at both the slow (3-4 days post attachment) and fast feeding phase (5-6 days post attachment), and ticks close to full repletion (7-9 days post attachment).

Double-stranded RNA synthesis and delivery

Double-stranded RNA was synthesized for hemocytin, cystatin, fibronectin and lipocalin for microinjection and gene silencing as previously described (9, 28).

RNA extraction, cDNA synthesis, and qRT-PCR

The samples utilized in this study have previously undergone confirmation of infection status in our previous study (10). The initial confirmation of *Ehrlichia* infection within these samples was conducted following established protocols (29). RNA was extracted from individual tissue using the Trizol-chloroform separation and isopropanol precipitation method. The quality of the isolated RNA was checked and stored at -80°C until use. Complementary DNA (cDNA) was synthesized from the isolated RNA as previously described (28). Briefly, the infection status was validated using an absolute quantification method and a standard curve of *E. chaffeensis* 16S rRNA to serve as the reference template for qRT-PCR.

Single hemocyte encapsulation

Three independent cohorts of adult female lone star ticks (*Amblyomma americanum)* representing unfed, blood-fed, and *Ehrlichia*-infected (Arkansas strain) ticks were prepared for

hemolymph collection. Hemolymph was collected from these three cohorts using our published method with slight modifications (9). Analyzing hemocytes from unfed, partially fed, and infected ticks using single-cell sequencing offers a comprehensive view of the physiological changes and host-pathogen interaction dynamics at different stages. Evaluating these stages holistically provides a detailed understanding of the intricate interplay between the cellular immune response to blood feeding and pathogen presence. Collected hemolymph was resuspended in Leibovitz's L-15 Medium supplemented with 50% BSA. Hemocyte suspension was filtered through a 40 μm cell strainer and centrifuged at 500 g for 3 min at 4°C. The hemocyte pellet was washed and centrifuged five times using 1 mL of ice-cold Leibovitz's L-15 Medium supplemented with 50% FBS. The final pellet was resuspended in 200 μL PBS supplemented with 5% BSA.

Library preparation and sequencing

Single cell samples were assessed for proper quality control metrics prior to library preparation. All samples were quantitated through the Invitrogen Countess 3 FL Automated Cell Counter (Invitrogen, Thermo Fisher Scientific, Waltham, MA, USA) using ReadyCount Green/Red Viability Stain (ReadyCount Green/Red Viability Stain) per manufactures' protocol with GFP filter. Samples were all greater than 90% viable with cell density averaging 1000 cells/ul. A total of 10000 cells per sample were used for downstream library preparation. Single cell samples were processed through the 10X Genomics Chromium Single Cell 3' protocol v3.1 per manufactures' instruction. Single cell droplets (GEMs) were produced using the 10X Genomics Chromium Controller and barcoded for sample identification. Final libraries were validated on the Qiagen QIAxcel DNA High Sensitivity Bioanalyzer (QIAGEN, Germantown, MD, USA)), to visualize proper insert size, and concentration was calculated using the KAPA Illumina Quantification Kit (Kapa Biosystems, Wilmington, MA, USA) on the Bio-Rad CFX96 thermal cycler (Bio-Rad Inc., Hercules, CA, USA). Pooled libraries were sequenced on the Illumina NextSeq 2000 per 10X Genomics specifications (28x91 cycles).

Quality control and data processing

The obtained raw single-cell sequencing dataset was analyzed for quality statistics using the official 10X Genomics analysis software Cell Ranger (10x Genomics, Cell Ranger 3.1.0). The forward and reverse reads were uploaded to the cell ranger cloud platform, and reference alignment was carried out on a custom-made reference file. When analyzing this data, no reference genome for A. americanum is available. To navigate this technical hurdle, we created a pseudo-genome using publicly available transcriptomes to generate contigs that were "stitched" with 50 N spacers in a pseudo-chromosome fasta (fa) file from which a general feature format (gtf) file was created (Supplementary Table S1). The short reads used for this assembly have the NCBI Short Reads Archive (SRA) accessions SRR1740607, SRR1740608, SRR1740609, SRR1740611, SRR1027751, SRR1027762, SRR1027471, SRR1027473, SRR1027474, SRR1027475, SRR1027476, SRR1027477, SRR1027479, SRR1027481, SRR1027483, SRR1027485, SRR1755762, SRR1756275, SRR1756327, SRR1756363, SRR1756401, SRR1756447, SRR1765066, SRR1755912, SRR1755757, SRR1765232, SRR1755874, SRR1755882, SRR1755921, SRR1755945, SRR1756279, SRR1756256, SRR1756263, SRR1756048, SRR1755913, SRR1756309, SRR1765128, SRR1765136, SRR1765151, SRR1755789, SRR1755723, SRR1765137, SRR1756448, SRR1756420, SRR1756431, SRR1756433, SRR1756139, SRR1755902, SRR1755922, SRR1756449, SRR1765217, SRR1755736, SRR1755893, SRR1765079, SRR1765248, SRR1755894, SRR1756287, SRR1765067, SRR1756059, SRR1755946, SRR1756101, SRR1756251, SRR1756280, SRR1756069, SRR1755923, SRR1764971, SRR1764999, SRR1755753, SRR4416250, SRR4416251, SRR4416252, SRR4416253, SRR4416254, SRR4416255, totaling 7,3 x 10^{10} bases. After trimming bases with low quality (less than 30) or matching Illumina primers, the reads were converted from fastq to fasta and normalized using the program insilico_read_normalization.pl from the Trinity package, allowing maximum coverage of 100 and smaller coverage of 5 (30). The normalized file served as input to the Abyss assembler (31) (with -k values of 20 – 90 in 10 x increments) and to the Trinity assembler. The resulting assemblies were combined into a single fasta file and clustered to 98% identity with the program CD-HIT-ESTs (32). The BUSCO version 5.0 (33) program running the Arachnida dataset against the assembled transcriptome file indicated 89.0% complete BUSCOs, of which 76.0% were complete and single copy, 13.0% were duplicated and 2.1% were fragmented, while 8.9% were missing out of 2,934 BUSCO genes. Since the assembled transcripts included hemocyte libraries, we estimate our gene coverage for the hemocyte-expressed transcripts was better than 90%. Finally, the CDSs were mapped to a hyperlinked Excel spreadsheet (Supplementary Table S2) containing matches to several databases, allowing an estimate of their functional classification.

Dimensionality reduction and cell clustering

The output matrices generated from the Cell Ranger software were loaded into the Seurat R package for cell clustering and dimensionality reduction analysis (34). Data were normalized using the 'LogNormalize' function, and the variations between cells were regressed by counting the number of target molecules in each cell, Unique Molecular Identifiers (UMI). Next, the scaled data underwent Principal Component Analysis (PCA) to reduce dimensionality. The JackStrawPlot function was utilized to examine the distribution of P-values. Among the PCA results, the principal component (PC) with the most significant statistical significance ($p < 10\text{-}5$) was chosen for subsequent clustering and cluster analysis

(35). Leveraging the identified PCs, cells were clustered and organized using the 'FindClusters' function. To further investigate data structures and cell trajectories, t-SNE and UMAP were employed, enabling separate visualization and exploration (36, 37).

Marker gene identification

The Seurat functions 'FindAllMarkers' and 'roc' were employed to identify marker genes associated with the obtained cell clusters. The marker gene refers to a set of genes used to identify and characterize identified hemocyte clusters within the cohorts. This analysis involved testing the cluster-enriched genes for significance. Subsequently, cluster-specific marker genes were subjected to additional screening criteria: they had to be expressed in over 50% of cells within a given cluster and exhibit an average natural log-fold change greater than 0.5. Multiple replicate analyses were conducted using either the same or different parameters to ensure the robustness and accuracy of the marker genes.

Pseudotemporal ordering of cells

Slingshot was used to comprehensively examine cell differentiation and fate. The data was transferred to the slingshot package by leveraging information from the identified cell clusters and differentially expressed genes. Subsequently, genes associated with cell differentiation and cell fate were selected to define the progression of cellular differentiation. Slingshot effectively reduced the dimensionality of the data to two dimensions and arranged all cells in a meaningful order. Genes exhibiting similar expression patterns, potentially indicating shared biological functions, were grouped together. The 'learning-graph' function was employed to calculate cell trajectories, providing insights into the progression of cellular differentiation.

Code availability

The generated data were analyzed using the 10X genomics Cell Ranger v7.1 (10x Genomics, Cell Ranger 3.1.0). Data analysis and visualization were carried out following the Seurat – Guided Clustering Tutorial (https://satijalab.org/seurat/articles/pbmc3k_tutorial.html) in R studio using all default settings.

Data availability

The raw datasets generated in this study are deposited in the NCBI Transcriptome Shotgun Annotation (TSA) repository under the accession number PRJNA226980. The pseudo-genome and pseudo-GTF files (Supplementary Table S1) can be downloaded from https://proj-bip-prod-publicread.s3.amazonaws.com/transcriptome/Amb_americanum_pseudogenome/amb_amer_pseudo_fa_gtf.zip

Supplementary Table S2 containing the assembled and annotated CDS can be downloaded from https://proj-bip-prod-publicread.s3.amazonaws.com/transcriptome/Amb_americanum_pseudogenome/Amb_amer-s2.zip

Results

Single cell RNA-seq of hemocytes from A. americanum

To examine hemocyte heterogeneity by scRNA-seq, isolated hemocytes from unfed, partially fed, and partially fed-*Ehrlichia chaffeensis* infected *A. americanum* ticks were subjected to the 10X Chromium Single Cell 3' sequencing platform. Approximately 27,130 cells (unfed: 6445; partially fed: 5847; partially fed *Ehrlichia*-infected: 14838) were captured using the 10X Genomics Chromium microfluidic technique and submitted to RNA sequencing. After standard pre-processing, a total of 26,040 cells covering 5870 cells from unfed, 5427 cells from partially blood-fed, and 14,744 cells from *Ehrlichia*-infected ticks were detected. A sequencing depth of ~14,000 reads per cell at a median sequence saturation of 69.6% (unfed), 67.9% (blood-fed), and 66.5% (*Ehrlichia* infected) across libraries were achieved. We obtained a median Unique Molecular Identifiers (UMI) and gene counts of 835 and 3181 from uninfected cohorts, 915 and 3478 from partially fed cohorts, and 582 and 2281 from partially fed-*Ehrlichia*-infected cohort (Figures 1A–C), respectively. Principal component linear dimensional reduction and the Uniform Manifold Approximation and Projection (UMAP) tool were used to visualize the filtered datasets (38, 39). We initially considered comparing uninfected, partially fed, and infected unfed cohorts but found variations in hemocyte clusters, making it hard to draw reliable conclusions. Due to this complexity, we integrated all three cohorts—unfed, partially fed, and infected ticks—into a single analysis. This approach provided a more comprehensive understanding of cellular dynamics across different stages, bypassing the difficulties observed when analyzing uninfected versus infected unfed ticks separately. Prior to unsupervised clustering, we applied the Seurat Integration batch correction method on all three cohorts. Seurat's unsupervised clustering analysis on the transformed cohort grouped hemocytes into fourteen clusters (Figure 2A) based on similar gene expression profiles (19, 20). For the comparison between the three conditions, each cluster had the following number of cells: Cluster 0 with 3903 cells (14.4%), Cluster 1 with 3727 cells (13.7%), Cluster 2 with 3210 cells (11.8%), Cluster 3 with 3045 cells (11.2%), Cluster 4 with 2846 cells (10.5%), Cluster 5 with 2422 cells (8.9%), Cluster 6 with 1715 cells (6.3%), Cluster 7 with 1452 cells (5.4%), Cluster 8 with 1259 cells (4.6%), Cluster 9 with 1226 cells (4.5%), Cluster 10 with 903 cells (3.3%), Cluster 11 with 799 cells (2.9%), Cluster 12 with 412 cells (1.5%), and Cluster 13 with 207 cells (0.8%) (Figure 2B). All cohorts appears to have equal proportion of cells represented across clusters, however, cells from *Ehrlichia*-infected cohorts represents more than 50% of cells in clusters 0, 2, 4, 5, 6, 7, 9, 11 and 12 (Figures 2C, D).

10.3389/fimmu.2023.1305976

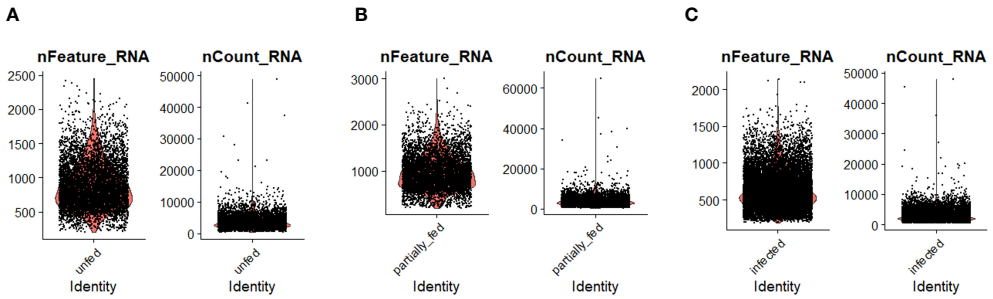

FIGURE 1
The distribution of the number of transcripts (nFeature_RNA) and genes (nCount_RNA) detected per hemocyte in **(A)** unfed, **(B)** partially fed, and **(C)** *Ehrlichia chaffeensis*-infected cohort.

Functional classification of hemocyte clusters

Seurat FindMarker function was used to identify the top 100 Differentially Expressed Genes (DEGs) in each cluster and functional assignment was carried out based on homology search in other tick species, UNIPROT, KOG, PFAM and SMART databases. The identified hemocyte clusters were characterized based on these functional assignments (Figure 2E, Supplementary Table S3). MEROPS classification of the proteases and protease inhibitors shows majority of the genes belonged to the putative bpti/kunitz family of serine protease inhibitor (I02.001), carboxypeptidase I inhibitor (S10.016), chymotrypsin-elastase inhibitor ixodidin (I08.001), metalloproteinase-1 (M10.001), cystatin (I25A), kunitz/bovine pancreatic trypsin inhibitor (I03.034), serine protease inhibitor (Family I4), and TIL domain-containing protein (I03.010).

Clusters 0, 5, and 9 display high expression of secreted genes with roles as protease inhibitors and cytoskeletal functions (Figure 2E). The marker genes in these clusters include a translation initiation factor 3 (14835), a metalloprotease (116223), lipocalins (16064, 146185, 90157), hemocytin (90421) and a serine protease inhibitor (137223), which are all involved in cellular and humoral immune response (Figure 2F).

The cells in cluster 1 express secreted genes involved in protein synthesis, protease inhibitors, metabolism, and immune response (Figure 2E). The identified metabolism genes are involved in lipid, amino acid and energy metabolism. The identified markers in this cluster include Inositol 1,4,5-trisphosphate receptor (120699; 120701), adenylyl cyclase (107091), serine protease inhibitor (31360), chymotrypsin inhibitor (105147), and carboxypeptidase inhibitor (76650). Inositol is involved in phagocytosis, and its expression induced via serotonin modulation. At the same time, serpin, chymotrypsin, and carboxypeptidase inhibitors have diverse roles in humoral immunity and blood digestion (Figure 2F).

Cluster 2 shares a similar functional expression of genes as in cluster 1 (Figure 2E); however, it is marked with high expression of marker genes such as mucin (459841) and cystatin (9505, 22377), which are all secreted proteins regulating immune response and chitinase (187500), which is involved in wound healing (Figure 2F).

Cluster 3 and 4 are enriched with genes with functions in nuclear regulation and cytoskeletal functions such as several histones (129995, 9657, 153147, 188513), GTPase-activating protein (81855, 77010), laminin (70101) and kinesin-like protein (195826) (Figure 2E). These genes are involved in the regulation of cell cycle, gene expression, cytoskeletal organization, and signal transduction. They are also components of the extracellular matrix (ECM) and basement membranes (BMs) and perform roles ranging from cell adhesion to cell-to-cell migration (Figure 2F).

Cluster 6 is enriched with secreted genes related to protein synthesis, protease inhibitors, metabolism, and detoxification (Figure 2E). The transcripts with metabolic functions in this cluster involve energy metabolism. The marker genes in this cluster include a glutathione S-transferase (175001), mitochondrial NADH: ubiquinone oxidoreductase (82400), and heat shock protein (58400). These genes are involved in the production of ROS and the regulation of oxidative stress. ROS is essential in wound healing cell differentiation and innate immunity (Figure 2F).

Cluster 7 showed high expression of genes related to protein synthesis, protease inhibitor, and metabolism (Figure 2E). Bulk of the metabolism genes in this cluster are involved in energy metabolism with few lipid and carbohydrate metabolism genes identified. The highly expressed marker genes include cytochrome_P450 (1455319), low-density lipoprotein receptor (58886), and cystatin-B (145319). These genes are involved in the cellular stress response, activation of lysosomal enzymes, lipoprotein metabolism, and protease degradation (Figure 2F).

Cluster 8 showed high expression of genes related to signal transduction, transcription machinery, immunity, and protein synthesis (Figure 2E). Such genes identified in this cluster include intersectin (102281), translation initiation factor IF-2 (1495781), hemocytin-like (113156) and calpain-b (98929). These genes are important regulators of cell transport, apoptosis regulation, and microbial binding and aggregation (Figure 2F).

Cluster 10 is enriched for secreted genes and genes cytoskeletal, transcriptional machinery, protein synthesis, protease inhibitor, and metabolic functions (Figure 2E). The marker genes in this cluster include cathepsin-L (89264), transforming growth factor-beta-induced protein ig-h3 (51103), soma ferritin (154941), a

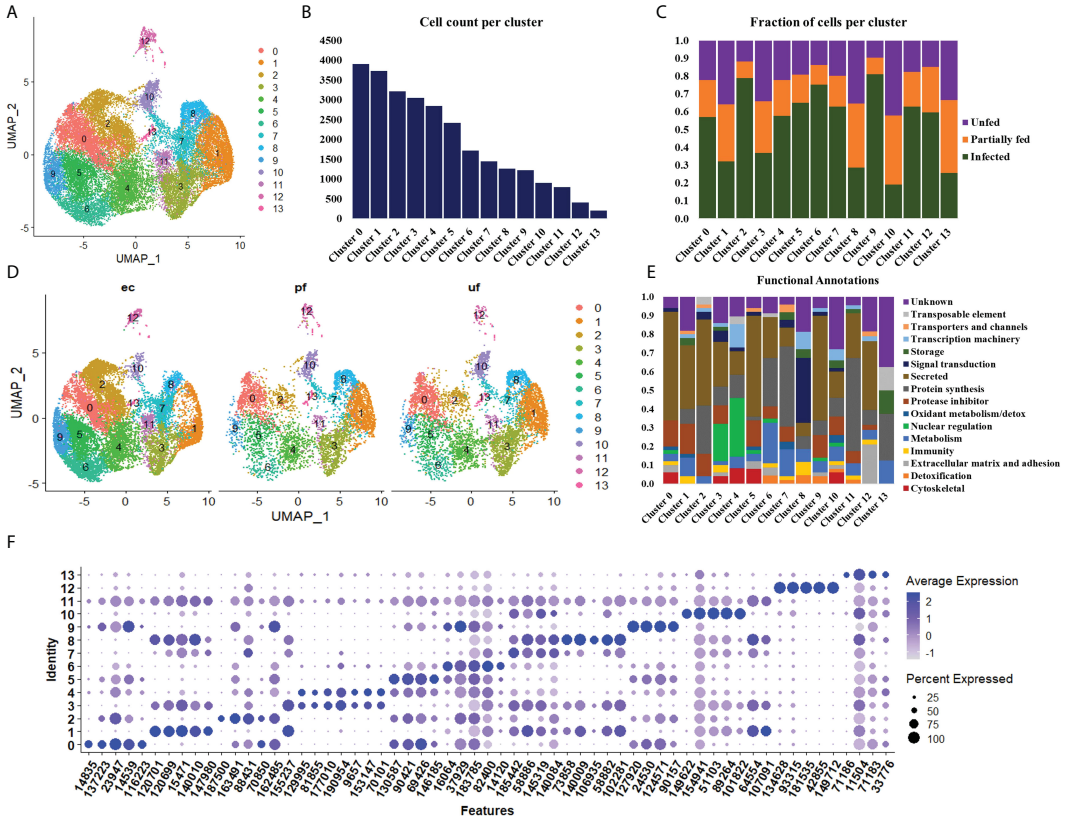

FIGURE 2
Uniform Manifold Approximation and Projection (UMAP) projection of hemocyte clusters identified from unfed, partially fed, and *Ehrlichia chaffeensis* infected *A. americanum* ticks **(A)**. Total number of cells in each Seurat cluster **(B)** and fraction of cells represented in each cluster from unfed, partially fed, and *Ehrlichia chaffeensis* infected ticks **(C)**. UMAP projection of the differences in cluster density in unfed, partially blood-fed, and *Ehrlichia chaffeensis* infected ticks **(D)** and functional annotation of hemocyte clusters using the top 100 DEGs **(E)**. Dot plot profiling of differentially expressed genes **(F)**. The color gradient of dots represents the expression level, while the size represents the percentage of cells expressing any genes per cluster.

putative peptidase inhibitor (1018222), and fibronectin (106951). These marker genes are involved in protein degradation, cell differentiation, transport, and cellular differentiation (Figure 2F).

Cluster 11 is enriched with genes involved in protein synthesis and secretory function, such as keratinocyte-associated protein 2 (125644), carboxypeptidase inhibitor (76650), and serine protease inhibitor (31360) (Figure 2E). The presence of these genes will suggest the role of this cluster in cytoskeletal binding, encapsulation, and tissue remodeling during repair (Figure 2F).

Cluster 12 has high expression of secreted genes and genes involved in protein synthesis and extracellular matrix and adhesion (Figure 2E). The marker genes in this cluster include cuticle protein (42855), transglutaminase substrate-like (181535), a glycine-rich protein (134628, hemicentin (933328), and reeler domain-containing protein (28024). The functional role of these genes involves the formation of the extracellular matrix and cuticle development, cell differentiation, and the formation of the peritrophic matrix (Figure 2F).

Cluster 13 has the least expressed number of genes and is not of hemocyte origin. However, functional enrichment showed the few genes detected are involved in storage, protein synthesis, and metabolic processes (Figures 2E, F).

Cell lineage analysis

We used slingshot to perform pseudotime analysis from the obtained hemocyte clusters to investigate the potential differentiation trajectory and reveal lineage relationships between the identified clusters. Seven hemocyte lineages were predicted. The first lineage starts from cluster 0 through clusters 5, 6, 4, 11, 7 and ends at cluster 1. The second lineage originates from cluster 0 through clusters 5, 6, 4, 11, 13 and ends at cluster 10. Lineage 3 originates from cluster 0 through clusters 5, 6, 4, 11, 13 and ends at cluster 12. Lineage 4 originates from cluster 0 through clusters 5, 6, 4, 11, 7 and ends at cluster 8. Lineage 5 originates from cluster 0 through clusters 5, 6, 4, 11 and ends at cluster 3. Lineage 6 originates from cluster 0 through clusters 5 and ends at cluster 9. Lineage 7 runs from cluster 0 and ends at cluster 2 (Figure 3).

Considering the lack of known hemocyte markers, we calculated and searched for highly expressed genes over pseudotime. However, we did not observe a unique association between the identified genes and distinct clusters or lineages, rather a group with multiple clusters (Figures 4A–D). We identified a putative soma ferritin gene (154941) which was differentiated in cluster 10 as part of lineage 2 (Figure 4A). A putative histone H4

(129995) is enriched in clusters 3, 4 and 11, which are components of lineage 5 (Figure 4B). The expression of a lipocalin-5 (16064) in clusters 5, 6, 9 is high compared to clusters 1, 3, and 11 (Figure 4C). A laminin (70101) transcript is enriched in clusters 3 and 4 (Figure 4D). In addition, differentially expressed genes that changes across lineages were identified. The genes include a ribosomal protein S16 (88431), a hypothetical secreted protein (23947), a translation initiation factor-2 (14835), a transposon (188473), lipocalin-5 (16064) and a chitinase-like lectin (187500) (Figures 5A–F). Seven lineages with shared clusters amongst multiple lineages indicate that many hemocyte populations display pluripotency and can differentiate into different cell types.

Marker genes contribute to hemocyte homeostasis and pathogen dissemination

We identified tick immune genes highly expressed in *E. chaffeensis*infected clusters. To investigate the role of these genes, the transcripts of hemocytin, cystatin, fibronectin, and lipocalin, which were depleted in *E. chaffeensis*infected adult female ticks by injecting double-stranded RNA. Quantitative real-time PCR confirmed significant transcript depletion of all genes tested from the hemolymph (Figures 6A–D). Hemocytin and lipocalin knockdown significantly reduced the total hemocyte population, while the hemocyte number increased in cystatin-silenced ticks. Hemocyte count, however, remained the same in fibronectin-silenced ticks (Figures 6F–H). We next quantified the different hemocyte populations between the knockdown and control groups. Silencing of hemocytin resulted in reduced granulocyte and plasmatocyte populations (Figures 7A–C). On the other hand, silencing cystatin led to an increased number of granulocytes and plasmatocytes (Figures 7D–F). The number of granulocytes decreased following fibronectin silencing (Figures 7G–I), while lipocalin silencing reduced prohemocytes and granulocyte populations (Figures 7J–L). These findings underscore the diverse and gene-specific contributions to hemocyte homeostasis, shedding light on the intricate regulation of the tick's immune response.

To further study how these immune genes contribute to the cellular immune response during pathogen infection, we quantified *E. chaffeensis* load in the hemolymph, salivary gland, and midguts isolated from silenced and control ticks. Our results showed that silencing hemocytin resulted in increased *Ehrlichia* load in the salivary gland (up one fold) and hemolymph (up 5 fold) (Figure 8A), while silencing of cystatin led to a decrease in *Ehrlichia* load in hemolymph and tissues (Figure 8B). Interestingly, silencing of fibronectin did not affect the *Ehrlichia* load (Figure 8C). In contrast, the pathogen load increased in lipocalin silenced tissues and hemolymph (Figure 8D). Together, these findings present a comprehensive understanding of how specific genes influence the tick's immune response to *E. chaffeensis* infection.

Discussion

The innate immune system of hematophagous arthropods is essential to their response to commensal and pathogen infection. We recently characterized the morphological changes and molecular responses of tick *A. maculatum* and *A. americanum* hemocytes to *R. parkeri* and *E. chaffeensis* infection (9, 10). However, technical challenges and the paucity of reagents related to characterized molecular markers limit functional studies on these cell types. In the current study, we sequenced hemocytes isolated from *A. americanum* ticks under unfed, partially fed, and *E. chaffeensis*-infected conditions using a single-cell approach. Our

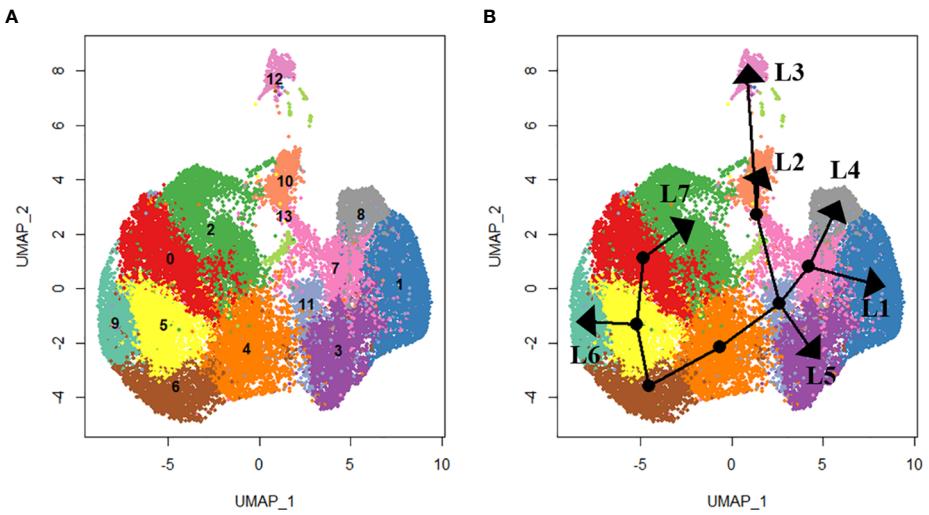

FIGURE 3
Lineage analysis using SlingShot. In total, seven lineages were identified as shown by the **(A)** UMAP projections of each cluster and **(B)** the respective lineage trajectory. Lineage 1 (L1) includes clusters 0. 5, 6, 4, 11, 7 and 1. Lineage 2 (L2) includes clusters 0, 5, 6, 4, 11, 13 and 10. Lineage 3 (L3) includes clusters 0, 5, 6, 4, 11, 13 and 12. Lineage 4 (L4) includes clusters 0, 5, 6, 4, 11, 7 and 8. Lineage 5 (L5) includes clusters 5, 6, 4, 11 and 3. Lineage 6 (L6) includes clusters 0, 5 and 9. Lineage 7 (L7) includes clusters 0 and 2.

10.3389/fimmu.2023.1305976

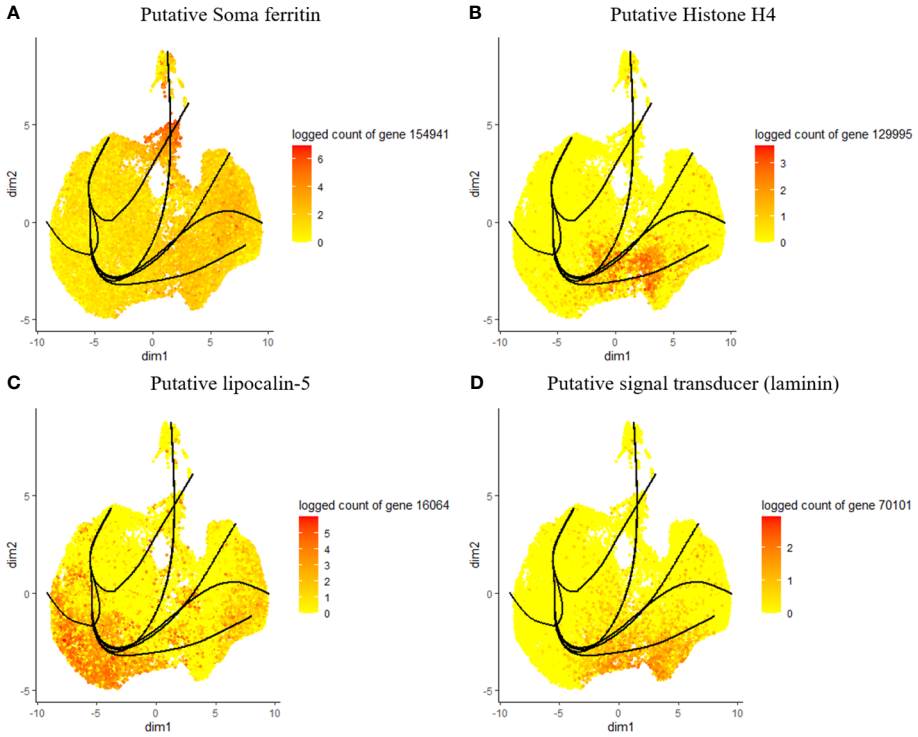

FIGURE 4
Expression of top genes, including putative soma ferritin **(A)**, putative histone h4 **(B)**, lipocalin-5 **(C)** and laminin **(D)** as their expression changes across pseudotime.

result showed extensive heterogeneity in hemocyte populations, with significant changes observed in hemocytes infected with intracellular tick-borne pathogens, *E. chaffeensis*.

This study identified 14 distinct hemocyte clusters, and the most notable changes in hemocyte population and cluster proportion were seen with *E. chaffeensis* infection. The clusters

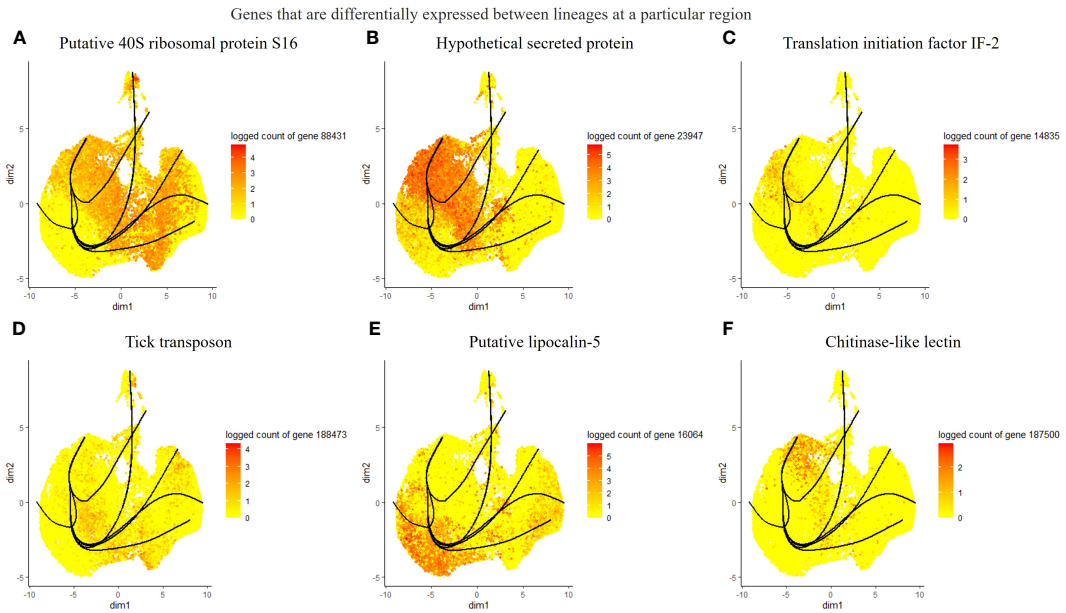

FIGURE 5
List of differentially expressed genes between lineages at different branches. The top 6 genes include a putative 40S ribosomal protein S16 **(A)**, a hypothetical protein **(B)**, translation initiation factor IF-2 **(C)**, tick transposon **(D)**, lipocalin-5 **(E)**, and chitinase-like-lectin **(F)**.

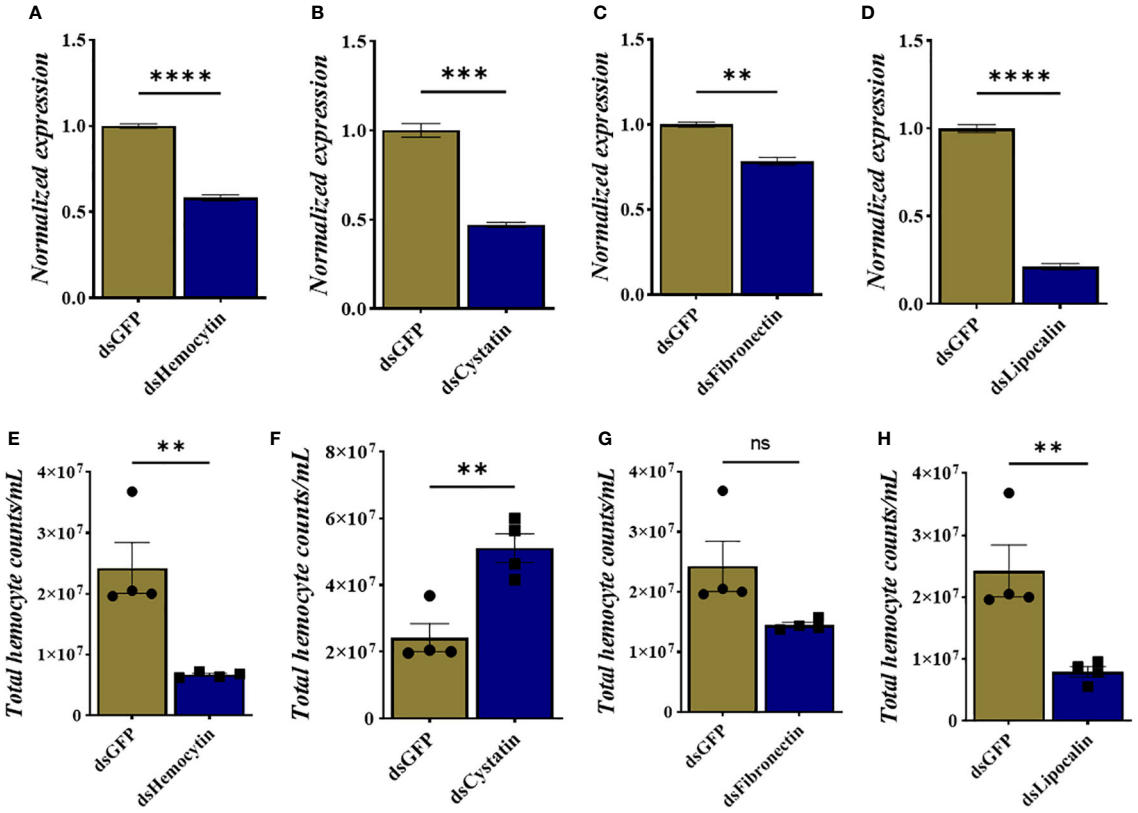

FIGURE 6
Knockdown of hemocyte marker genes results in changes in total hemocyte population. **(A–D)** Depletion of marker gene transcript following dsRNA injection and **(E–H)** total hemocyte numbers in each silenced gene. Gene expression was normalized to A. americanum actin. Data was analyzed using an unpaired t-test in GraphPad Prism 8.4.1. Asterisks denote significance (*P < 0.05, **P < 0.01, ***P < 0.001, ****P < 0.0001).

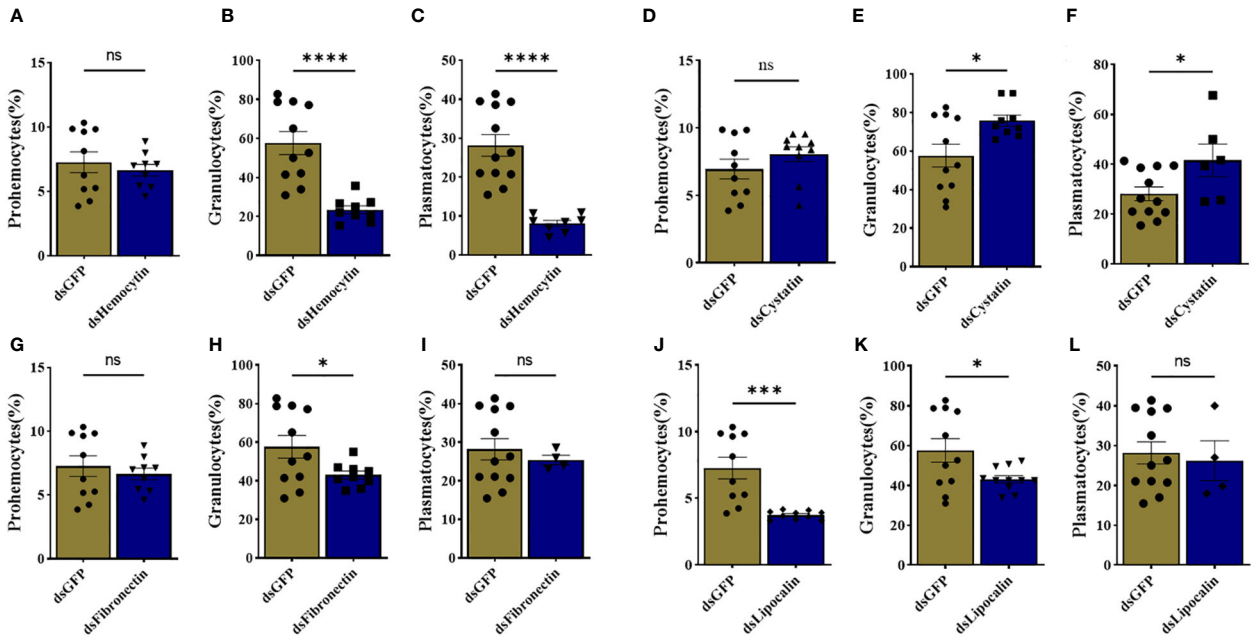

FIGURE 7
Knockdown of marker genes disrupts overall hemocyte homeostasis. Estimated percentage of prohemocytes, granulocytes, and plasmatocytes from **(A-C)** hemocytin, **(D-F)** cystatin, **(G-I)** fibronectin, and **(J-L)** lipocalin silenced ticks. Data was analyzed using an unpaired t-test in GraphPad Prism 8.4.1. Asterisks denote significance (*P < 0.05, ***P < 0.001, ****P < 0.0001).

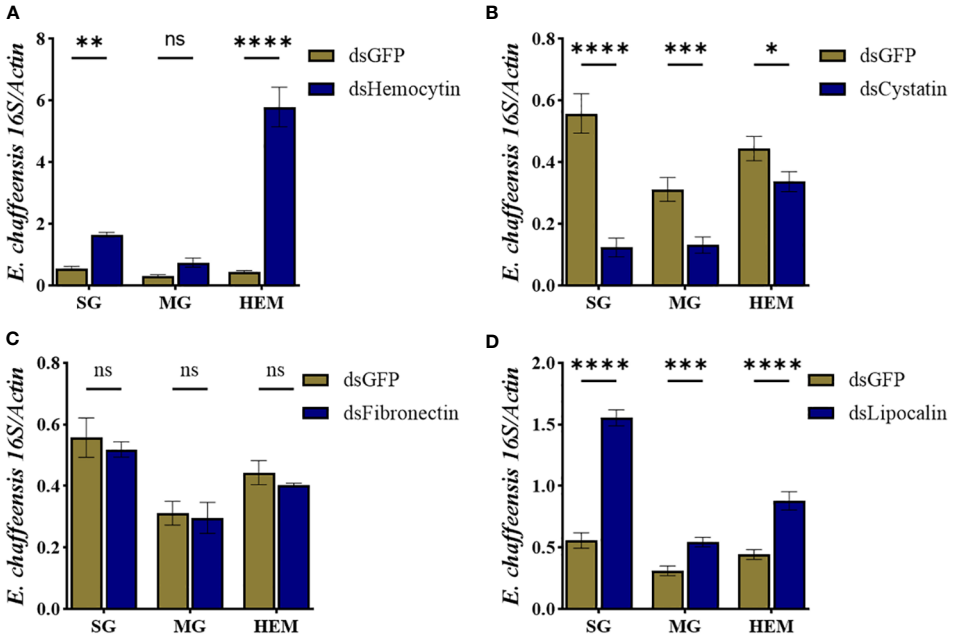

FIGURE 8
Hemocyte markers genes contribute to *Ehrlichia chaffeensis* infection. *Ehrlichia chaffeensis* burden in salivary gland, midgut, and hemolymph isolated from **(A)** hemocytin, **(B)** cystatin, **(C)** fibronectin, and **(D)** lipocalin silenced ticks. Data was analyzed using an unpaired t-test in GraphPad Prism 8.4.1. Asterisks denote significance (*P < 0.05, **P < 0.01, ***P < 0.001, ****P < 0.0001).

with a fraction of cells induced by *E. chaffeensis* infection were notable for their expression of genes involved in cytoskeletal functions, nuclear regulation, protein synthesis, metabolism, detoxification, and extracellular matrix secretion. Interestingly, these clusters are shared across three different lineages, 4, 6, and 7, suggesting a common ancestry among the cells from these clusters. The genes expressed in these clusters are involved in microbial recognition and agglutination, cellular differentiation and proliferation, and response to oxidative stress.

Considering the difficulty in functionally characterizing the role of the identified genes in hemocyte functions, we focused on those genes that are highly abundant in clusters enriched in *E. chaffeensis*-infected cohorts. These genes include hemocytin, chitinase-like proteins, serine-protease inhibitors, lipocalins, cystatins, heat shock proteins, and glutathione s-transferase. In addition, we identified genes that are involved in regulating cellular immune response and cellular differentiation. These include histones, laminins, GTPase, and kinesin.

Hemocytin, an orthologs of *Drosophila* hemolectin and human von Willebrand factor, is an adhesive protein released from the granules of granulocytic hemocytes via exocytosis and is the first step in the formation of nodules after infection (40–42). Chitinase-like proteins (CLPs) belong to the glycoside hydrolase family 18 (GH18). CLPs expression upregulated in *Drosophila* following injury, parasitic infection and bacterial infection by inducing clot formation and wound healing (43–46). Serine-protease inhibitors serve as pattern recognition proteins and are also components of the prophenoloxidase (proPO)-activating system, a major humoral defense mechanism in arthropods (47–50). The role of these genes as components of the immune response and their expression in hemocyte clusters enriched in *E. chaffeensis* infected cohorts is indicative of their contribution to the immune response during *E. chaffeensis* infection. Considering the role of these genes in microbial binding, the clusters in which they are enriched (0, 5, and 9) could be regarded as involved in pattern recognition.

Lipocalins are also involved in the transport of small molecules across biological barriers. No direct evidence exists for their role in hemocyte-mediated immunity or their hemocyte-specific expression; however, an *Anopheles (A) gambiae* lipocalin serves as a carrier molecule for a hemocyte differentiator factor, which subsequently leads to immune priming (51). Alignment of the lipocalin sequences revealed that 67% to 99% amino acid identify with other tick lipocalins (Supplementary Figure 1; Supplementary Table S4) containing the histamine binding motif found in tick salivary proteins. The top hits belonged to sequences from *A. americanum, A. sculptum, A. aureolatum, R. haemaphysaloides*, and *A. maculatum* (Supplementary Figure 1; Supplementary Table S4). It is interesting to note that the three *A. maculatum* (Amac-hemSigP-446830, Amac-hemSigP-446831, and AmHem-446832) transcripts were hemocyte-specific transcripts from *A. maculatum* (9). Tick lipocalins perform immunomodulatory roles during tick feeding by scavenging and binding histamines and other biogenic amines (52, 53). Tick lipocalins are functionally diverse, with little sequence identified across tick species. This diversity is also specie dependent as certain tick species, such as *A. maculatum, A. americanum*, reportedly have 170 and 200 lipocalin coding sequences, while species like *H. longicornis* and *I. persulcatus* have just 1 and 12 lipocalin CDS in their genomes (54). In *A. americanum*, 200 lipocalin coding sequences are present, constituting approximately 27% of the whole transcriptome in the

salivary gland (55). Similarly, the expression of multiple lipocalin transcripts changes throughout tick feeding, suggesting a time-dependent specificity even in the same tick species (28). Lipocalin expression also changes in response to pathogen infection (56). A lipocalin isolated from *Ornithodoros savignyi* showed distinct expression in the hemocytes and midgut following bacterial infection and blood-feeding, respectively, suggesting a tissue-dependent role for lipocalins (57). Tick lipocalins reportedly bind to serotonin and serotonin-binding proteins (53, 58, 59). Serotonin and serotonin receptors are responsible for the phagocytic response seen in *Drosophila* and the caterpillar, *Pieris (P) rapae* (60) and also in the aggregation of hemocytes and nodule formation in *B. mori* (42). The affinity of tick lipocalin towards serotonin or other serotonin-binding proteins would suggest their role in defense response against pathogens with their high expression of multiple lipocalin transcripts in clusters enriched in *E. chaffeensis* infected cohorts.

Cystatins are stored inside the granules of granulocytic hemocytes and possess strong AMP activities against Gram-negative bacteria (61). The cystatin transcripts from this study were 33-71% identical with previously studied cystatins from other tick species (Supplementary Figure 2; Supplementary Table S5), with the most identity has been salivary cystatin-L from *Hyalomma asiaticum*, *R. sanguineus, R. microplus, Dermacentor (D) silvarum*, and *D. andersoni* (Supplementary Figure 2; Supplementary Table S5). Cystatins are a family of proteins that play important roles in regulating protease activity by inhibiting cysteine proteases, such as Cathepsins, in various biological processes. In ticks, cystatins have unique properties and functions primarily related to tick feeding and evasion of the host immune response. Tick cystatins are essential for the tick's ability to feed on the host's blood and inhibit proteases involved in host immune responses (62–66). Similarly, ticks secrete cystatins during tick-borne pathogen infection and colonization. Tick cystatins can inhibit cysteine proteases produced by pathogens, as demonstrated in *R. microplus* during *B. microti* colonization (67). The expression of multiple cystatin transcripts was upregulated in *R. microplus* salivary gland infected with *Theileria equi* (68). In addition to their presence in salivary gland and midgut, tick hemocytes express high levels of cystatins, suggesting a role in innate immune response (14, 69, 70). The remarkable diversity and tissue specificity of tick cystatins contribute to their multifaceted roles in tick physiology. Negative regulation of the tick immune system has been described for tick cystatins. Knockdown of *Rmcystatin*, a cystatin from *Rhipicephalus (R) microplus*, rendered ticks immunocompetent upon bacterial infection (69). A similar observation was made in the pacific oyster, *C. gigas*, where an enhanced bacterial clearance was detected following the knockdown of the cystatin *CgCytA* (71). Our data identified cystatin as a marker in two clusters enriched in *E. chaffeensis*-infected cohorts. *E. chaffeensis* may induce cystatin expression to evade immune response since cystatin can inhibit several proteases found in hemocyte granules (72).

The expression of laminins, histones, kinesins, and GTPase is unique to clusters 3 and 4. However, while all three cohorts share relatively equal proportions of cells in cluster 3, *E. chaffeensis* infected cohorts have a higher fraction of cells from cluster 4 than the unfed and partially fed cohorts. Histones are indispensable for the organization and architecture of chromatin, and their post-translational modifications play a vital role in gene regulation (73). However, they also possess antimicrobial activities against bacteria, fungi, viruses, and protozoa (74). In vertebrates, they act as damage-associated molecular patterns (DAMPs) and bind to pattern recognition receptors (PRRs), which eventually trigger the innate immune response (75). Histones are components of extracellular traps (ETs) granulocytes produced upon microbial infection (76). Granulocyte-produced extracellular traps of *Periplaneta (P) americana* comprised DNA and histones, and the ETs contribute to granulocyte-mediated nodulation following bacterial infection (76). Laminins are components of extracellular matrix (ECM) and basement membranes (BMs). They interact with cell-surface molecules and other ECM components and perform roles ranging from cell adhesion to cell-to-cell migration. In *Drosophila*, laminins are produced by embryonic hemocytes, which are required for hemocyte migration (77). Laminins also play vital roles in hemocyte homeostasis, as silencing a laminin receptor decreased the hemocyte population in *Penaeus (Litopenaeus) vannamei* (78). GTPase plays a crucial role in biological processes such as cell cycle regulation, gene expression, cytoskeletal organization, and signal transduction (79). In invertebrates, Rac1, a member of the Rho GTPase family, was highly expressed in the hemocytes of the Chinese shrimp *Fenneropenaeus chinensis*, and the expression was upregulated following viral infection (80). Several kinesin-like proteins play a role in chromosomal segregation and congression during meiosis (81, 82). Due to their involvement in microtubule dynamics, they are required for efficient phagocytosis (83). The high expression profiles of these genes enriched in all cohorts and those enriched in *E. chaffeensis* cohorts, as seen in cluster 3 and cluster 4, respectively, imply that these genes contribute to hemocyte homeostasis and proliferation, as seen with histones and laminins. In addition, they also have additional functions in response to infection and act as migration factors for hemocytes via cytoskeletal reorganization and antimicrobial compounds. When considered together, clusters 3 and 4 may be similar hemocyte populations demonstrating plasticity upon infection.

Glutathione S-transferase and heat shock proteins are highly expressed in cluster 6, enriched in *E. chaffeensis*-infected cohort. Glutathione S-transferases (GSTs) are enzymes that regulate redox homeostasis, detoxification, and innate immune responses against bacterial infection. Multiple sequence alignment of the GST sequence from this study shows identity ranging from 53%-86% identity with most similar sequences coming from *R. microplus, D. andersoni, D. silvarum, D. asiaticum, R. sanguineus, H. longicornis* and *I. scapularis* (Supplementary Figure 3; Supplementary Table S6). GST expression is associated with oxidative stress response and immune response activation (84, 85). Increased expression of GSTs in ticks is associated with the detoxification of acaricides (86). Increased hemocyte expression is associated with induction with bacterial components such as LPS or peptidoglycan (87) or virus

infection (88). GTSs also encode enzymes that detoxify Drosophila's hydrogen peroxide and lipid peroxidases (89, 90). ROS production in the hemocytes is required during the early phase of infection for hemocyte activation and bacterial clearance (84). A *Drosophila* GST-S1 was reported to induce an increase in larval hemocytes (91), and the expression of GST-S1 was also increased in hemocytes during early metamorphosis (92), suggesting a functional role in regulating hemocyte proliferation. The expression of tick GSTs is associated with blood feeding in response to elevated oxidative stress. Breakdown of blood meals results in high levels of ROS, thus acting as a signal transducer for the expression of GSTs (93, 94). Increased expression of tick GSTs during blood meal is shown in *I. ricinus* and *R. microplus* (95, 96). In the midgut, transport, and intracellular digestion of heme in the midgut epithelial results in continuous ROS production throughout feeding, resulting in the upregulation of multiple GST transcripts (97). The expression of GST in tick salivary gland is seen towards the late stage of feeding, which coincides with salivary gland degeneration and massive release of intracellular salivary proteins into the salivary ducts (98, 99). Other studies have also reported multiple GST transcripts in the salivary gland, ovaries, and fat bodies; however, these GST transcripts gradually reduce as ticks move towards full engorgement (100). Heat shock proteins (HSP) are associated with elevated stress levels and act as chaperones during high protein turnover or degradation. In invertebrates, elevated levels of HSPs in hemocytes are associated with increased oxidative stress, usually associated with wounding or infection (101, 102). Elevated levels of reactive oxygen species (ROS) and associated oxidative stress during melanization or clotting response to sterile or contaminated wounds (103). The role of both GST and HSP in stress metabolism and cell protection during both blood feeding and infection makes them an integral component of the immune response, further emphasizing their high expression in *E. chaffeensis-infected* cohorts.

Initial efforts to study the function of selected hemocyte markers revealed possible dynamic roles for these genes. Silencing hemocytin, fibronectin, lipocalin, and cystatin impacts the overall hemocyte population, suggesting a role in maintaining homeostasis within the tick vector. Perhaps the most intriguing finding in the context of this study is the specificity at which silencing these genes impacts *Ehrlichia* infection in the whole tick. We found that silencing hemocytin and lipocalin resulted in a higher pathogen load, which interestingly correlates to decreased granulocytes and plasmatocyte count. Hemocytin is differentially expressed in *R. parkeri*-infected *A. maculatum* hemocytes (9). A recent study also showed an increased *Anaplasma phagocytophilum* load in hemocytin-silenced tick (23), further supporting our observation. These results support that hemocytin is an essential component of the tick cellular immune response and is required for regulating intracellular pathogen infection within the tick vector. In contrast to hemocytin knockdown, silencing lipocalin suppresses pathogen replication in tissues and hemolymph. We observed a significant drop in prohemocyte counts and a slightly reduced granulocyte count in lipocalin-silenced ticks.

In conclusion, we used single-cell transcriptome to delineate hemocyte heterogeneity in a blood-feeding arthropod. We identified 14 unique hemocyte clusters and revealed changes in cluster population induced by *E. chaffeensis*. The findings here serve as a significant resource to generate new knowledge to understand tick immune biology and their responses to microbial infection.

Limitations

This study has led to the identification of several hemocyte-derived genes that can be used to define hemocyte populations. Using pseudotime and trajectory analysis has identified several potential genes that will be useful in determining hemocyte pluripotency into other hemocyte types. However, the lack of an annotated *A. americanum* genome and hemocyte transcriptome limited our ability to make conclusive inferences. While our study aims to provide insights into hemocyte changes under unfed, partially fed and infected conditions, we recognize that the data presented might not fully encapsulate all the events during tick feeding. Future investigations could consider longitudinal studies capturing a broader temporal range to elucidate better the dynamic changes that occur throughout the feeding and infection process. Nonetheless, these findings offer valuable insights into hemocyte-molecular signatures, contributing to understanding hemocyte biology and overall tick physiology at these stages.

Data availability statement

The raw single-cell RNA sequences were deposited into the NCBI Sequence Read Archive (SRA) repository under the BioProject ID PRJNA1060745.

Ethics statement

The animal study was reviewed and approved by the University of Southern Mississippi's Institutional Animal Care and Use Committee (USMIACUC protocols #15101501.3 and 17101206.2). The study was conducted in accordance with the local legislation and institutional requirements.

Author contributions

AA: Conceptualization, Formal analysis, Investigation, Methodology, Writing – original draft, Writing – review & editing. JR: Data curation, Formal analysis, Resources, Writing – review & editing. RS: Data curation, Formal analysis, Investigation, Methodology, Writing – review & editing. SK: Conceptualization, Funding acquisition, Investigation, Project administration, Resources, Supervision, Writing – original draft, Writing – review & editing.

Funding

The author(s) declare financial support was received for the research, authorship, and/or publication of this article. This research was principally supported by the NIH NIAID Awards #R15AI167013, #R21AI175885, and # RO1AI163857. We thank the UMMC Molecular and Genomics facility, supported by the NIH-NIGMS (#P20GM103476 & P20GM144041). JR was supported by the Intramural Research Program of the NIAID (Vector-Borne Diseases: Biology of Vector Host Relationship, Z01 AI000810-18). The funders played no role in the study design, data collection, analysis, publication, decision, or manuscript preparation.

Acknowledgments

This work utilized the computational resources of the NIH HPC Biowulf cluster (http://hpc.nih.gov).

Conflict of interest

The authors declare that the research was conducted in the absence of any commercial or financial relationships that could be construed as a potential conflict of interest.

The author(s) declared that they were an editorial board member of Frontiers, at the time of submission. This had no impact on the peer review process and the final decision.

Publisher's note

Supplementary material

The Supplementary Material for this article can be found online at: https://www.frontiersin.org/articles/10.3389/fimmu.2023.1305976/full#supplementary-material

SUPPLEMENTARY FIGURE 1
The neighbor-joining phylogenetic tree from the aligned lipocalin sequences following 1000 bootstraps. The bar at the bottom represents 20% amino acid diversity. The numbers at the nodes indicate the percentage bootstrap support.

SUPPLEMENTARY FIGURE 2
The neighbor-joining phylogenetic tree from the aligned cystatin sequences following 1000 bootstraps. The bar at the bottom represents 20% amino acid diversity. The numbers at the nodes indicate the percentage bootstrap support.

SUPPLEMENTARY FIGURE 3
The neighbor-joining phylogenetic tree from the aligned glutathione s-transferase sequences following 1000 bootstraps. The bar at the bottom represents 20% amino acid diversity. The numbers at the nodes indicate the percentage bootstrap support.

SUPPLEMENTARY SHEET 1
NCBI short reads from short reads archive (SRA) and their accessions used for transcripts assembly.

SUPPLEMENTARY SHEET 2
Base statistics of the short reads used.

SUPPLEMENTARY SHEET 3
Combined coding sequences matched to publicly available databases.

SUPPLEMENTARY SHEET 4
Multiple alignment of lipocalin protein sequences using Constraint-based Multiple Alignment (COLBALT).

SUPPLEMENTARY SHEET 5
Multiple alignment of cystatin protein sequences using Constraint-based Multiple Alignment (COLBALT).

SUPPLEMENTARY SHEET 6
Multiple alignment of glutathione s-transferase protein sequences using Constraint-based Multiple Alignment (COLBALT). Multiple alignment of protein sequences using Constraint-based Multiple Alignment (COLBALT).

References

1. Inoue N, Hanada K, Tsuji N, Igarashi I, Nagasawa H, Mikami T, et al. Characterization of phagocytic hemocytes in Ornithodoros moubata (Acari: Ixodidae). *J Med Entomol* (2001) 38(4):514–9. doi: 10.1603/0022-2585-38.4.514

2. Mondekova HH, Sima R, Urbanova V, Kovar V, Ryan RO, Grubhoffer L, et al. Characterization of Ixodes ricinus fibrinogen-related proteins (Ixoderins) discloses their function in the tick innate immunity. *Front Cell Infect Microbiol* (2017) 509:509. doi: 10.3389/fcimb.2017.00509

3. Urbanová V, Hajdušek O, Hönig Mondeková H, Šíma R, Kopáček P. Tick Thioester-Containing Proteins and Phagocytosis Do Not Affect Transmission of Borrelia afzelii from the Competent Vector Ixodes ricinus. *Front Cell Infect Microbiol* (2017) 7:73. doi: 10.3389/fcimb.2017.00073

4. Pereira LS, Oliveira PL, Barja-Fidalgo C, Daffre S. Production of reactive oxygen species by hemocytes from the cattle tick Boophilus microplus. *Exp Parasitol* (2001) 99 (2):66–72. doi: 10.1006/expr.2001.4657

5. Fogaça AC, Almeida IC, Eberlin MN, Tanaka AS, Bulet P, Daffre S. Ixodidin, a novel antimicrobial peptide from the hemocytes of the cattle tick Boophilus microplus with inhibitory activity against serine proteinases. *Peptides* (2006) 27(4):667–74. doi: 10.1016/j.peptides.2005.07.013

6. Kocan KM, de la Fuente J, Manzano-Roman R, Naranjo V, Hynes WL, Sonenshine DE. Silencing expression of the defensin, varisin, in male Dermacentor variabilis by RNA interference results in reduced Anaplasma marginale infections. *Exp Appl Acarol* (2008) 46(1–4):17–28. doi: 10.1007/s10493-008-9159-5

7. Feitosa APS, Chaves MM, Veras DL, de Deus DMV, Portela NC, Araújo AR, et al. Assessing the cellular and humoral immune response in Rhipicephalus sanguineus sensu lato (Acari: Ixodidae) infected with Leishmania infantum (Nicolle 1908). *Ticks Tick Borne Dis* (2018) 9(6):1421–30. doi: 10.1016/j.ttbdis.2018.06.007

8. Fiorotti J, Urbanová V, Gôlo PS, Bittencourt VREP, Kopáček P. The role of complement in the tick cellular immune defense against the entomopathogenic fungus Metarhizium robertsii. *Dev Comp Immunol* (2022) 126:104234. doi: 10.1016/j.dci.2021.104234

9. Adegoke A, Ribeiro JMC, Brown S, Smith RC, Karim S. Rickettsia parkeri hijacks tick hemocytes to manipulate cellular and humoral transcriptional responses. *Front Immunol* (2023) 14:1094326. doi: 10.3389/fimmu.2023.1094326

10. Adegoke A, Julian H, Smith RC, Karim S. *Ehrlichia chaffeensis* co-opts phagocytic hemocytes for systemic dissemination in the Lone Star tick, *Amblyomma americanum*. (2023). doi: 10.1101/2023.08.17.553720

11. Binnington KC, Obenchain FD. Structure and Function of the Circulatory, Nervous and Neuroendocrine Systems of Ticks. In: *Physiology of ticks*. (Elsevier: Pergamon Press) (1982) 351–98. Obenchain FD, Gakun R (Eds.). (2013). Biology of ticks volume 2 (Vol. 2). Oxford University Press.

12. Borovičková B, Hypša V. Ontogeny of tick hemocytes: A comparative analysis of ixodes ricinus and Ornithodoros moubata. *Exp Appl Acarol* (2005) 35(4):317–33. doi: 10.1007/s10493-004-2209-8

13. Sonenshine DE, Michael RE. *Biology of Ticks Volume 2 (2nd ed.)*. Oxford University Press. (2013). Available at: https://global.oup.com/academic/product/biology-of-ticks-volume-2-9780199744060?cc=us&lang=en&.

14. Mao F, Wong NK, Lin Y, Zhang X, Liu K, Huang M, et al. Transcriptomic Evidence Reveals the Molecular Basis for Functional Differentiation of Hemocytes in a Marine Invertebrate, Crassostrea gigas. *Front Immunol.* (2020) 11:911. doi: 10.3389/fimmu.2020.00911

15. Cattenoz PB, Sakr R, Pavlidaki A, Delaporte C, Riba A, Molina N, et al. Temporal specificity and heterogeneity of Drosophila immune cells. *EMBO J* (2020) 39(12):e104486. doi: 10.15252/embj.2020104486

16. Cho B, Yoon SH, Lee D, Koranteng F, Tattikota SG, Cha N, et al. Single-cell transcriptome maps of myeloid blood cell lineages in Drosophila. *Nat Commun* (2020) 11(1):4483. doi: 10.1038/s41467-020-18135-y

17. Tattikota SG, Cho B, Liu Y, Hu Y, Barrera V, Steinbaugh MJ, et al. A single-cell survey of Drosophila blood. *Elife* (2020) 9:e54818. doi: 10.7554/eLife.54818

18. Severo MS, Landry JJM, Lindquist RL, Goosmann C, Brinkmann V, Collier P, et al. Unbiased classification of mosquito blood cells by single-cell genomics and high-content imaging. *Proc Natl Acad Sci U S A* (2018) 115(32):E7568–77. doi: 10.1073/pnas.1803062115

19. Raddi G, Barletta ABF, Efremova M, Ramirez JL, Cantera R, Teichmann SA, et al. Mosquito cellular immunity at single-cell resolution. *Science* (2020) 369(6507):1128–32. doi: 10.1126/science.abc0322

20. Kwon H, Mohammed M, Franzén O, Ankarklev J, Smith RC. Single-cell analysis of mosquito hemocytes identifies signatures of immune cell subtypes and cell differentiation. *Elife* (2021) 10:e66192. doi: 10.7554/eLife.66192

21. Feng M, Xia J, Fei S, Peng R, Wang X, Zhou Y, et al. Identification of silkworm hemocyte subsets and analysis of their response to baculovirus infection based on single-cell RNA sequencing. *Front Immunol* (2021) 12:645359. doi: 10.3389/fimmu.2021.645359

22. Feng M, Swevers L, Sun J. Hemocyte Clusters Defined by scRNA-Seq in Bombyx mori: In Silico Analysis of Predicted Marker Genes and Implications for Potential Functional Roles. *Front Immunol* (2022) 13:852702. doi: 10.3389/fimmu.2022.852702

23. Rolandelli A, Laukaitis-Yousey HJ, Bogale HN, Singh N, Samaddar S, O'Neal AJ, et al. Tick hemocytes have pleiotropic roles in microbial infection and arthropod fitness. *bioRxiv [Preprint]* (2023). doi: 10.1101/2023.08.31.555785

24. Koiwai K, Koyama T, Tsuda S, Toyoda A, Kikuchi K, Suzuki H, et al. Single-cell RNA-seq analysis reveals penaeid shrimp hemocyte subpopulations and cell differentiation process. *Elife* (2021) 10:e66954. doi: 10.7554/eLife.66954

25. Cui C, Tang X, Xing J, Sheng X, Chi H, Zhan W. Single-cell RNA-seq uncovered hemocyte functional subtypes and their differentiational characteristics and connectivity with morphological subpopulations in Litopenaeus vannamei. *Front Immunol* (2022) 13:980021. doi: 10.3389/fimmu.2022.980021

26. Pichon R, Pinaud S, Vignal E, Chaparro C, Pratlong M, Portet A, et al. Single cell RNA sequencing reveals hemocyte heterogeneity in Biomphalaria glabrata: Plasticity over diversity. *Front Immunol* (2022) 13:956871. doi: 10.3389/fimmu.2022.956871

27. Karim S, Browning R, Ali L, Truhett R. Laboratory-infected Ehrlichia chaffeensis female adult Amblyomma americanum salivary glands reveal differential gene expression. *J Med Entomol* (2012) 49(3):547–54. doi: 10.1603/me11214

28. Bullard R, Allen P, Chao CC, Douglas J, Das P, Morgan SE, et al. Structural characterization of tick cement cones collected from in *vivo* and artificial membrane blood-fed Lone Star ticks (Amblyomma americanum). *Ticks Tick Borne Dis* (2016) 7(5):880–92. doi: 10.1016/j.ttbdis.2016.04.006

29. Teymournejad O, Lin M, Rikihisa Y. Ehrlichia chaffeensis and its invasin EtpE block reactive oxygen species generation by macrophages in a DNase X-dependent manner. *mBio* (2017) 8(6):e01551–17. doi: 10.1128/mBio.01551-17

30. Haas BJ, Papanicolaou A, Yassour M, Grabherr M, Blood PD, Bowden J, et al. *De novo* transcript sequence reconstruction from RNA-seq using the Trinity platform for reference generation and analysis. *Nat Protoc* (2013) 8(8):1494–512. doi: 10.1038/nprot.2013.084

31. Simpson JT, Wong K, Jackman SD, Schein JE, Jones SJ, Birol I. ABySS: a parallel assembler for short read sequence data. *Genome Res* (2009) 19(6):1117–23. doi: 10.1101/gr.089532.108

32. Li W, Godzik A. Cd-hit: a fast program for clustering and comparing large sets of protein or nucleotide sequences. *Bioinformatics* (2006) 22(13):1658–9. doi: 10.1093/bioinformatics/btl158

33. Simão FA, Waterhouse RM, Ioannidis P, Kriventseva EV, Zdobnov EM. BUSCO: assessing genome assembly and annotation completeness with single-copy orthologs. *Bioinformatics* (2015) 31(19):3210–2. doi: 10.1093/bioinformatics/btv351

34. Hao Y, Hao S, Andersen-Nissen E, Mauck WM 3rd, Zheng S, Butler A, et al. Integrated analysis of multimodal single-cell data. *Cell* (2021) 184(13):3573–87. doi: 10.1016/j.cell.2021.04.048

35. Chung NC, Storey JD. Statistical significance of variables driving systematic variation in high-dimensional data. *Bioinformatics* (2015) 31(4):545–54. doi: 10.1093/bioinformatics/btu674

36. McDavid A, Finak G, Chattopadyay PK, Dominguez M, Lamoreaux L, Ma SS, et al. Data exploration, quality control and testing in single-cell qPCR-based gene expression experiments. *Bioinformatics* (2013) 29(4):461–7. doi: 10.1093/bioinformatics/bts714

37. Perrin D, Zuccon G. Recursive module extraction using Louvain and PageRank. *F1000Res* (2018) 7:1286. doi: 10.12688/f1000research.15845.1

38. Becht E, McInnes L, Healy J, Dutertre CA, Kwok IWH, Ng LG, et al. Dimensionality reduction for visualizing single-cell data using UMAP. *Nat Biotechnol* (2018). doi: 10.1038/nbt.4314

39. Stuart T, Butler A, Hoffman P, Hafemeister C, Papalexi E, Mauck WM 3rd, et al. Comprehensive integration of single-cell data. *Cell* (2019) 177(7):1888–1902.e21. doi: 10.1016/j.cell.2019.05.031

40. Ratcliffe NA, Gagen SJ. Studies on the in *vivo* cellular reactions of insects: an ultrastructural analysis of nodule formation in Galleria mellonella. *Tissue Cell* (1977) 9(1):73–85. doi: 10.1016/0040-8166(77)90050-7

41. Arai I, Ohta M, Suzuki A, Tanaka S, Yoshizawa Y, Sato R. Immunohistochemical analysis of the role of hemocytin in nodule formation in the larvae of the silkworm, Bombyx mori. *J Insect Sci* (2013) 13:125. doi: 10.1673/031.013.12501

42. Otuka H, Sato R. Serotonin- and eicosanoid-dependent rapid hemocyte aggregation in the hemolymph is the first step in nodule formation in Bombyx mori larvae. *J Insect Physiol* (2023) 145:104486. doi: 10.1016/j.jinsphys.2023.104486

43. De Gregorio E, Spellman PT, Rubin GM, Lemaitre B. Genome-wide analysis of the Drosophila immune response by using oligonucleotide microarrays. *Proc Natl Acad Sci U S A* (2001) 98(22):12590–5. doi: 10.1073/pnas.221458698

44. Irving P, Troxler L, Heuer TS, Belvin M, Kopczynski C, Reichhart JM, et al. A genome-wide analysis of immune responses in Drosophila. *Proc Natl Acad Sci U S A* (2001) 98(26):15119–24. doi: 10.1073/pnas.261573998

45. Kucerova L, Broz V, Arefin B, Maaroufi HO, Hurychova J, Strnad H, et al. The drosophila chitinase-like protein IDGF3 is involved in protection against nematodes and in wound healing. *J Innate Immun* (2016) 8(2):199–210. doi: 10.1159/000442351

46. De Gregorio E, Spellman PT, Tzou P, Rubin GM, Lemaitre B. The Toll and Imd pathways are the major regulators of the immune response in Drosophila. *EMBO J* (2002) 21(11):2568–79. doi: 10.1093/emboj/21.11.2568

47. Cerenius L, Söderhäll K. The prophenoloxidase-activating system in invertebrates. *Immunol Rev* (2004) 198:116–26. doi: 10.1111/j.0105-2896.2004.00116.x

48. Iwanaga S, Lee BL. Recent advances in the innate immunity of invertebrate animals. *J Biochem Mol Biol* (2005) 38(2):128–50. doi: 10.5483/bmbrep.2005.38.2.128

49. Jiravanichpaisal P, Lee BL, Söderhäll K. Cell-mediated immunity in arthropods: hematopoiesis, coagulation, melanization and opsonization. *Immunobiology* (2006) 211(4):213–36. doi: 10.1016/j.imbio.2005.10.015

50. Cerenius L, Lee BL, Söderhäll K. The proPO-system: pros and cons for its role in invertebrate immunity. *Trends Immunol* (2008) 29(6):263–71. doi: 10.1016/j.it.2008.02.009

51. Ramirez JL, de Almeida Oliveira G, Calvo E, Dalli J, Colas RA, Serhan CN, et al. A mosquito lipoxin/lipocalin complex mediates innate immune priming in Anopheles Gambiae. *Nat Commun* (2015) 6:7403. doi: 10.1038/ncomms8403

52. Paesen GC, Adams PL, Nuttall PA, Stuart DL. Tick histamine-binding proteins: lipocalins with a second binding cavity. *Biochim Biophys Acta* (2000) 1482(1-2):92–101. doi: 10.1016/s0167-4838(00)00168-0

53. Mans BJ, Ribeiro JM. A novel clade of cysteinyl leukotriene scavengers in soft ticks. *Insect Biochem Mol Biol* (2008) 38(9):862–70. doi: 10.1016/j.ibmb.2008.06.002

54. Ribeiro JMC, Bayona-Vásquez NJ, Budachetri K, Kumar D, Frederick JC, Tahir F, et al. A draft of the genome of the Gulf Coast tick, Amblyomma maculatum. *Ticks Tick Borne Dis* (2023) 14(2):102090. doi: 10.1016/j.ttbdis.2022.102090

55. Karim S, Ribeiro JM. An Insight into the Sialome of the Lone Star Tick, Amblyomma americanum, with a Glimpse on Its Time Dependent Gene Expression. *PloS One* (2015) 10(7):e0131292. doi: 10.1371/journal.pone.0131292

56. Ribeiro JM, Alarcon-Chaidez F, Francischetti IM, Mans BJ, Mather TN, Valenzuela JG, et al. An annotated catalog of salivary gland transcripts from Ixodes scapularis ticks. *Insect Biochem Mol Biol* (2006) 36(2):111–29. doi: 10.1016/j.ibmb.2005.11.005

57. Cheng PH, Mans BJ, Neitz AW, Gaspar AR. Savicalin, a lipocalin from hemocytes of the soft tick, Ornithodoros savignyi. *Exp Appl Acarol* (2010) 52(3):313–26. doi: 10.1007/s10493-010-9368-6

58. Sangamnatdej S, Paesen GC, Slovak M, Nuttall PA. A high affinity serotonin- and histamine-binding lipocalin from tick saliva. *Insect Mol Biol* (2002) 11(1):79–86. doi: 10.1046/j.0962-1075.2001.00311.x

59. Mans BJ, Ribeiro JM, Andersen JF. Structure, function, and evolution of biogenic amine-binding proteins in soft ticks. *J Biol Chem* (2008) 283(27):18721–33. doi: 10.1074/jbc.M800188200

60. Qi YX, Huang J, Li MQ, Wu YS, Xia RY, Ye GY. Serotonin modulates insect hemocyte phagocytosis via two different serotonin receptors. *Elife* (2016) 5:e12241. doi: 10.7554/eLife.12241

61. Agarwala KL, Kawabata S, Hirata M, Miyagi M, Tsunasawa S, Iwanaga S. A cysteine protease inhibitor stored in the large granules of horseshoe crab hemocytes:

purification, characterization, cDNA cloning and tissue localization. *J Biochem* (1996) 19(1):85–94. doi: 10.1093/oxfordjournals.jbchem.a021220

62. Karim S, Miller NJ, Valenzuela J, Sauer JR, Mather TN. RNAi-mediated gene silencing to assess the role of synaptobrevin and cystatin in tick blood feeding. *Biochem Biophys Res Commun* (2005) 334(4):1336–42. doi: 10.1016/j.bbrc.2005.07.036

63. Kotsyfakis M, Karim S, Andersen JF, Mather TN, Ribeiro JM. Selective cysteine protease inhibition contributes to blood-feeding success of the tick Ixodes scapularis. *J Biol Chem* (2007) 282(40):29256–63. doi: 10.1074/jbc.M703143200

64. Lu S, da Rocha LA, Torquato RJS, da Silva Vaz Junior I, Florin-Christensen M, Tanaka AS. A novel type 1 cystatin involved in the regulation of Rhipicephalus microplus midgut cysteine proteases. *Ticks Tick Borne Dis* (2020) 11(3):101374. doi: 10.1016/j.ttbdis.2020.101374

65. Parizi LF, Rangel CK, Sabadin GA, Saggin BF, Kiio I, Xavier MA, et al. Rhipicephalus microplus cystatin as a potential cross-protective tick vaccine against Rhipicephalus appendiculatus. *Ticks Tick Borne Dis* (2020) 11(3):101378. doi: 10.1016/j.ttbdis.2020.101378

66. Kotál J, Buša M, Urbanová V, Řezáčová P, Chmelař J, Langhansová H, et al. Mialostatin, a novel midgut cystatin from Ixodes ricinus ticks: crystal structure and regulation of host blood digestion. *Int J Mol Sci* (2021) 22(10):5371. doi: 10.3390/ijms22105371

67. Wei N, Du Y, Lu J, Zhou Y, Cao J, Zhang H, et al. A cysteine protease of Babesia microti and its interaction with tick cystatins. *Parasitol Res* (2020) 119(9):3013–22. doi: 10.1007/s00436-020-06818-w

68. Paulino P, Vitari G, Rezende A, Couto J, Antunes S, Domingos A, et al. Characterization of the Rhipicephalus (Boophilus) microplus Sialotranscriptome Profile in Response to Theileria equi Infection. *Pathogens* (2021) 10(2):167. doi: 10.3390/pathogens10020167

69. Lu S, Soares TS, Vaz Junior IS, Lovato DV, Tanaka AS. Rmcystatin3, a cysteine protease inhibitor from Rhipicephalus microplus hemocytes involved in immune response. *Biochimie* (2014) 106:17–23. doi: 10.1016/j.biochi.2014.07.012

70. Zhou J, Ueda M, Umemiya R, Battsetseg B, Boldbaatar D, Xuan X, et al. A secreted cystatin from the tick Haemaphysalis longicornis and its distinct expression patterns in relation to innate immunity. *Insect Biochem Mol Biol* (2006) 36(7):527–35. doi: 10.1016/j.ibmb.2006.03.003

71. Mao W, Liu S, Wang K, Wang M, Shi H, Liu Q, et al. Cystatin C in evaluating renal function in ureteral calculi hydronephrosis in adults. *Kidney Blood Press Res* (2020) 45(1):109–21. doi: 10.1159/000504441

72. Haves-Zburof D, Paperna T, Gour-Lavie A, Mandel I, Glass-Marmor L, Miller A. Cathepsins and their endogenous inhibitors cystatins: expression and modulation in multiple sclerosis. *J Cell Mol Med* (2011) 15(11):2421–9. doi: 10.1111/j.1582-4934.2010.01229.x

73. Parseghian MH, Luhrs KA. Beyond the walls of the nucleus: the role of histones in cellular signaling and innate immunity. *Biochem Cell Biol* (2006) 84(4):589–604. doi: 10.1139/o06-082

74. Kawasaki H, Iwamuro S. Potential roles of histones in host defense as antimicrobial agents. *Infect Disord Drug Targets* (2008) 8(3):195–205. doi: 10.2174/1871526510808030195

75. Li Z, Li D, Li Y, Guo X, Yang R. Deciphering the regulatory code of histone modifications in plants. *J Genet Genomics* (2022) 49(11):1064–7. doi: 10.1016/j.jgg.2022.07.003

76. Nascimento MTC, Silva KP, Garcia MCF, Medeiros MN, MaChado EA, Nascimento SB, et al. DNA extracellular traps are part of the immune repertoire of Periplaneta americana. *Dev Comp Immunol* (2018) 84:62–70. doi: 10.1016/j.dci.2018.01.012

77. Sánchez-Sánchez BJ, Urbano JM, Comber K, Dragu A, Wood W, Stramer B, et al. Drosophila embryonic hemocytes produce laminins to strengthen migratory response. *Cell Rep* (2017) 21(6):1461–70. doi: 10.1016/j.celrep.2017.10.047

78. Charoensapsri W, Sangsuriya P, Lertwimol T, Gangnonngiw W, Phiwsaiya K, Senapin S. Laminin receptor protein is implicated in hemocyte homeostasis for the whiteleg shrimp Penaeus (Litopenaeus) vannamei. *Dev Comp Immunol* (2015) 51(1):39–47. doi: 10.1016/j.dci.2015.02.012

79. Hall A. Rho family GTPases. *Biochem Soc Trans* (2012) 40(6):1378–82. doi: 10.1042/BST20120103

80. Chi Y, Li F, Sun Y, Wen R, Li S. Expression and function analysis of Rac1 homolog in Chinese shrimp Fenneropenaeus chinensis. *Fish Shellfish Immunol* (2013) 35(3):927–32. doi: 10.1016/j.fsi.2013.07.006

81. Mayr MI, Hümmer S, Bormann J, Grüner T, Adio S, Woehlke G, et al. The human kinesin Kif18A is a motile microtubule depolymerase essential for chromosome congression. *Curr Biol* (2007) 17(6):488–98. doi: 10.1016/j.cub.2007.02.036

82. Zhang P, Dai W, Hahn J, Gilbert SP. Drosophila Ncd reveals an evolutionarily conserved powerstroke mechanism for homodimeric and heterodimeric kinesin-14s. *Proc Natl Acad Sci U S A* (2015) 112(20):6359–64. doi: 10.1073/pnas.1505531112

83. Silver KE, Harrison RE. Kinesin 5B is necessary for delivery of membrane and receptors during FcγR-mediated phagocytosis. *J Immunol* (2011) 186(2):816–25. doi: 10.4049/jimmunol.1002161

84. Myers AL, Harris CM, Choe KM, Brennan CA. Inflammatory production of reactive oxygen species by Drosophila hemocytes activates cellular immune defenses. *Biochem Biophys Res Commun* (2018) 505(3):726–32. doi: 10.1016/j.bbrc.2018.09.126

85. Ramond E, Dudzic JP, Lemaitre B. Comparative RNA-Seq analyses of Drosophila plasmatocytes reveal gene specific signatures in response to clean injury and septic injury. *PloS One* (2020) 15(6):e0235294. doi: 10.1371/journal.pone.0235294

86. Hernandez EP, Kusakisako K, Talactac MR, Galay RL, Hatta T, Matsuo T, et al. Characterization and expression analysis of a newly identified glutathione S-transferase of the hard tick Haemaphysalis longicornis during blood-feeding. *Parasit Vectors* (2018) 11(1):91. doi: 10.1186/s13071-018-2667-1

87. Yang J, Wei X, Xu J, Yang D, Liu X, Yang J, et al. A sigma-class glutathione S-transferase from Solen grandis that responded to microorganism glycan and organic contaminants. *Fish Shellfish Immunol* (2012) 32(6):1198–204. doi: 10.1016/j.fsi.2012.03.010

88. Duan Y, Liu P, Li J, Li J, Chen P. Expression profiles of selenium dependent glutathione peroxidase and glutathione S-transferase from Exopalaemon carinicauda in response to Vibrio Anguillarum and WSSV challenge. *Fish Shellfish Immunol* (2013) 35(3):661–70. doi: 10.1016/j.fsi.2013.05.016

89. Singh SP, Coronella JA, Benes H, Cochrane BJ, Zimniak P. Catalytic function of Drosophila melanogaster glutathione S-transferase DmGSTS1-1 (GST-2) in conjugation of lipid peroxidation end products. *Eur J Biochem* (2001) 268(10):2912–23. doi: 10.1046/j.1432-1327.2001.02179.x

90. Saisawang C, Wongsantichon J, Ketterman AJ. A preliminary characterization of the cytosolic glutathione transferase proteome from Drosophila melanogaster. *Biochem J.* (2012) 442(1):181–90. doi: 10.1042/BJ20111747

91. Stofanko M, Kwon SY, Badenhorst P. A misexpression screen to identify regulators of Drosophila larval hemocyte development. *Genetics* (2008) 180(1):253–67. doi: 10.1534/genetics.108.089094

92. Regan JC, Brandão AS, Leitão AB, Mantas Dias AR, Sucena E, Jacinto A, et al. Steroid hormone signaling is essential to regulate innate immune cells and fight bacterial infection in Drosophila. *PloS Pathog* (2013) 9(10):e1003720. doi: 10.1371/journal.ppat.1003720

93. Daniel V. Glutathione S-transferases: gene structure and regulation of expression. *Crit Rev Biochem Mol Biol* (1993) 28(3):173–207. doi: 10.3109/10409239309086794

94. Dreher-Lesnick SM, Mulenga A, Simser JA, Azad AF. Differential expression of two glutathione S-transferases identified from the American dog tick, Dermacentor variabilis. *Insect Mol Biol* (2006) 15(4):445–53. doi: 10.1111/j.1365-2583.2006.00657.x

95. Rosa de Lima MF, Sanchez Ferreira CA, Joaquim de Freitas DR, Valenzuela JG, Masuda A. Cloning and partial characterization of a Boophilus microplus (Acari: Ixodidae) glutathione S-transferase. *Insect Biochem Mol Biol* (2002) 32(7):747–54. doi: 10.1016/s0965-1748(01)00157-6

96. Rudenko N, Golovchenko M, Edwards MJ, Grubhoffer L. Differential expression of Ixodes ricinus tick genes induced by blood feeding or Borrelia burgdorferi infection. *J Med Entomol* (2005) 42(1):36–41. doi: 10.1093/jmedent/42.1.36

97. Perner J, Provazník J, Schrenková J, Urbanová V, Ribeiro JM, Kopáček P. RNA-seq analyses of the midgut from blood- and serum-fed Ixodes ricinus ticks. *Sci Rep* (2016) 6:36695. doi: 10.1038/srep36695

98. Radulović ŽM, Kim TK, Porter LM, Sze SH, Lewis L, Mulenga A. A 24-48 h fed Amblyomma americanum tick saliva immuno-proteome. *BMC Genomics* (2014) 15:518. doi: 10.1186/1471-2164-15-518

99. Tirloni L, Islam MS, Kim TK, Diedrich JK, Yates JR 3rd, Pinto AF, et al. Saliva from nymph and adult females of Haemaphysalis longicornis: a proteomic study. *Parasit Vectors* (2015) 8:338. doi: 10.1186/s13071-015-0918-y

100. Hernandez EP, Talactac MR, Vitor RJS, Yoshii K, Tanaka T. An Ixodes scapularis glutathione S-transferase plays a role in cell survival and viability during Langat virus infection of a tick cell line. *Acta Trop* (2021) 214:105763. doi: 10.1016/j.actatropica.2020.105763

101. Chakrabarti S, Visweswariah SS. Intramacrophage ROS primes the innate immune system via JAK/STAT and toll activation. *Cell Rep* (2020) 33(6):108368. doi: 10.1016/j.celrep.2020.108368

102. Wrońska AK, Boguś MI. Heat shock proteins (HSP 90, 70, 60, and 27) in Galleria mellonella (Lepidoptera) hemolymph are affected by infection with Conidiobolus coronatus (Entomophthorales). *PloS One* (2020) 15(2):e0228556. doi: 10.1371/journal.pone.0228556

103. Krautz R, Arefin B, Theopold U. Damage signals in the insect immune response. *Front Plant Sci* (2014) 5:342. doi: 10.3389/fpls.2014.00342